



Interaction between a screw dislocation and an elastic elliptical inhomogeneity by using the angular basis function

J. T. Chen, J. W. Lee and S. K. Kao

Abstract. The behavior of displacement field due to a screw dislocation is similar to the angular basis function (ABF) $\text{Arg}(z)$. It is different from the radial basis function (RBF) $\ln(r)$ that is used to describe the velocity potential of a sink or source. Nevertheless, the complex-valued fundamental solution $\ln(z)$ contains the two parts of RBF $\ln(r)$ and ABF $\text{Arg}(z)$. In this paper, not only the RBF in the null-field boundary integral equation (BIE) but also the ABF for the screw dislocation are employed to study the interaction between a screw dislocation and an elastic elliptical inhomogeneity. This problem is decomposed into a free field with a screw dislocation and a boundary value problem containing an elliptical inhomogeneity. The boundary value problem is solved by using the RBF and the null-field BIE. Since the geometric shape is an ellipse, the degenerate kernel is expanded to a series form under the elliptical coordinates, while the unknown boundary densities are expanded to eigenfunctions. By combining the degenerate kernel and the null-field BIE, the boundary value problem can be easily solved. The inconsistency between Sendecykj (In: Simmons JA, et al (eds) *Fundamental aspects of dislocation theory*. US National Bureau of Standards, Gaithersburg, pp 57–69, 1970) and Gong and Meguid (Int J Eng Sci 32(8):1221–1228, 1994) for the problem was also found by using the present approach. The error in Gong and Meguid (Int J Eng Sci 32(8):1221–1228, 1994) was also printed out. Finally, some examples are demonstrated to verify the validity of the present approach.

Mathematics Subject Classification. 45-02.

Keywords. Angular basis function, Screw dislocation, Degenerate kernel, Null-field boundary integral equation.

1. Introduction

For the development of advanced materials, the interaction between a dislocation and multi-phase materials is an important topic. Two basic types are edge and screw dislocations. They are characterized by that the Burgers vector which is perpendicular and parallel with respect to the dislocation line, respectively. Many researchers investigated the dislocation and inclusion problems in the past years. Head [3] used an analogy between screw dislocations and electrostatic line charges to solve the interaction of an elastic screw dislocation with an idealized grain boundary. In the same year, the interaction between an edge dislocation and bimetallic elastic solid was reduced to two standard problems in potential theory by him [4]. Based on the technique of conformal mapping and the method of analytical continuation in conjunction with the alternating technique, Chen et al. [5] derived the analytical solution for plane elasticity problems of an elliptically cylindrical layered media subject to an arbitrary edge dislocation. Zhou et al. [6] reviewed recent works about inclusions well. Smith [7] successfully solved the problem of the interaction between a screw dislocation and a circular inclusion contained within an infinite body by using the complex-variable function and the circle theorem. Besides, the uniform anti-plane remote shear was also considered at the same time. Shen [8] used the complex variable theory and the alternating technique to deal with the problem of a circular layered inclusion interacting with a generalized screw dislocation under the remote anti-plane shear stress and in-plane magnetoelectric loads. In the same year, Wang and Pan also study this interaction between a screw dislocation and a viscoelastic piezoelectric

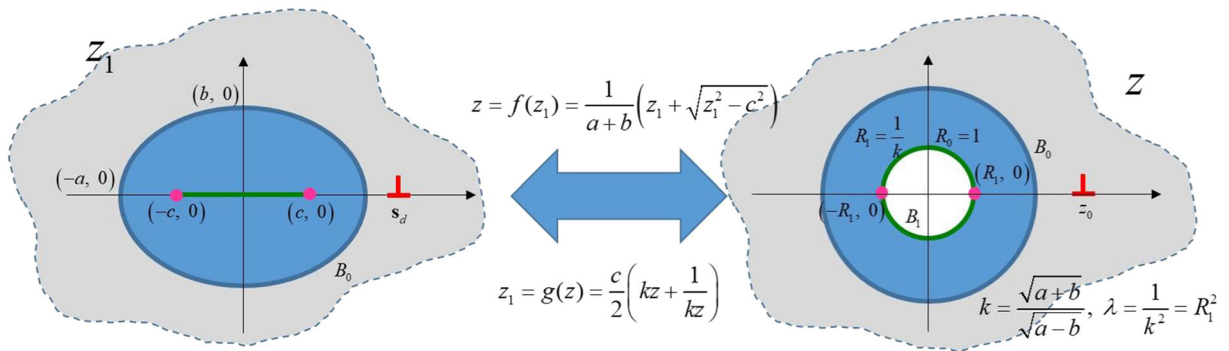


FIG. 1. An elliptical inhomogeneity and its mapped region

bimaterial interface [9]. Although Smith [7] introduced the conformal mapping to discuss the elliptical inhomogeneity, it exists a paradox. The ellipse would be mapped to concentric circles instead of a circle as shown in Fig. 1. The inner circular boundary must be considered. Later, Sendekyj [1] found that the five dislocations would be brought by this mapping operator as shown in Fig. 2. It violates the condition of only one dislocation. Sendekyj [1] introduced the corresponding dislocations to eliminate the extra dislocations. Gong and Meguid [2] revisited this problem in 1994. They used the Laurent series to represent the potential. Unfortunately, their analytical results of the potential function are not equivalent. The inconsistency may be attributed to typos. It is why we revisit this issue by using the alternative way, the angular basis function. This method is free of using the extra dislocations or matching the extra boundary condition to modify the potential. In this paper, we would examine this nonequivalence. Dislocation problems have been solved by using complex variables [10–12]. Fang et al. [13] derived the general solutions for the complex multiply connected region. Not only a screw dislocation but also interfacial cracks are considered for an elliptical inhomogeneity. Later, Luo and Xiao [14] investigated the nano inhomogeneity by accounting the Gurtin–Murdoch model. Recently, Wang and Schiavone [15] solved the interaction problem of a screw dislocation in an elastic inhomogeneity of arbitrary shape partially penetrated by a semi-infinite crack. For Burgers vector and the Peach–Koehler force, Lubarda [16] had a well-done review in 2019. Since almost all of the above problems were solved by using the complex-variable technique, its extension to three-dimensional cases may be limited. A more general approach is not trivial for further investigation. The present approach may fill the gap.

The complex-valued fundamental solution $\ln(z)$ can be decomposed into the radial basis function (RBF) and the angular basis function (ABF). Kansa [17] directly collocated the RBF to solve the parabolic, hyperbolic and the elliptic Poisson’s equation. Zheng et al. [18] proposed a meshless local RBF collocation method to calculate the band structures of 2D anti-plane transverse elastic waves in photonic crystals. The RBF was used to interpolate the data as well as to solve the PDE in recent decades [19–23]. Since the conventional fundamental solution is also one kernel of the RBF, e.g., $\ln r$, the expression to degenerate kernel provides an analytical tool to solve the problem. Chen et al. [20] employed the degenerate kernel and superposition technique to revisit the Green’s function of Laplace problems with circular boundaries. They derived the analytical solution by using the addition theorem free of the complex variables and the image method. Here, we introduce the degenerate (or so-called separable) kernel for the angle-type fundamental solution instead of the radial-basis one to represent the screw dislocation solution. The terminology of degenerate kernel is not coined by authors, but can refer to the literature [24]. To our best knowledge, the degenerate kernel for the angle-type fundamental solution was first proposed for the circular inclusion using the polar coordinates in [25]. After that, many researchers paid attention to the angle-type fundamental solution. In 2015, Young et al. [26] used the ABF to solve potential flow

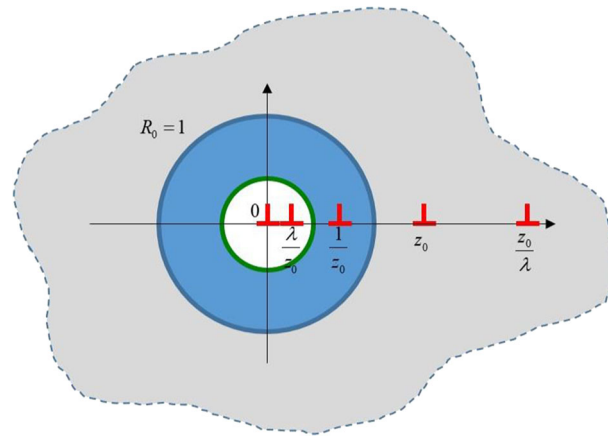


FIG. 2. Locations of the propagated dislocations through the mapping operator

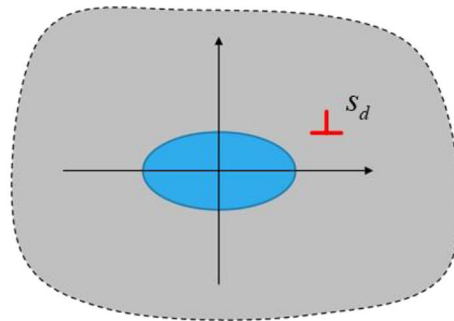
problems. However, a branch-cut problem may result in the difficulty in choosing the location of screw dislocation. Until 2018, Li et al. [27] proposed a new approach (MTABF) that can directly adopt source point distributions used in the traditional MFS to improve the method of angular basis function (MABF) proposed by Young et al. [26]. In the same year, Alves et al. [28] proposed a remedy which used a pair of two points to restrict the discontinuity appearing only along the line segment between two points, and they named this kind of singularity as cracklets. It is nothing more than the constant element of double-layer potential from the viewpoint of the dual BEM [29]. Kuo et al. [30] revisited the two-point angular basis functions (cracklets) and adopted the concept of domain decomposition or added the logarithmic function into the base function to deal with the problem of a multiply-connected domain with cracklets. Regarding the mathematical theory of dislocation, two books [31, 32] can be consulted with. In 1988, Hong and Chen [29] linked the bridge between the dual boundary integral equation and dislocation theory. Leandro [33] used the tangential differential operator to reduce the order of strong singularities in the traction BIE. Later, Liu and Li [34] revisited this equivalence and connected to the displacement discontinuity method.

Although previous investigations did a lot of elegant work for the problem of a screw dislocation, it seems that numerical results were very few in the literature. In this paper, we extend the previous success of a circular case [25] to an elliptical inclusion subject to a screw dislocation. The interaction between a screw dislocation and an elliptical inhomogeneity contained within an infinite body is demonstrated as shown in Fig. 3a. The angle-type fundamental solution for the screw dislocation in terms of degenerate kernel for polar coordinates is extended to the elliptical coordinates. The use of the degenerate kernel has the merit of free of singular integrals even collocating on the boundary of a domain. By employing the superposition technique, a screw dislocation solution is decomposed into two parts: one is the infinite plane subject to the screw dislocation problem, the other is the infinite plane with an elliptical inhomogeneity subject to the corresponding boundary condition. After superimposing the two solutions, the governing equation and boundary conditions can be both satisfied. Finally, the result is demonstrated to show the validity of the present method. Agreement with Sendekyj's result [1] is obtained. The typo of Gong and Meguid [2] is also verified.

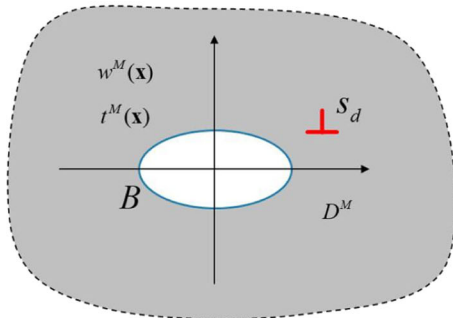
2. Problem statements

For the anti-plane strain problem, we only consider the anti-plane displacement w such that

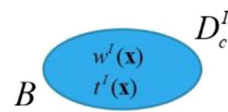
$$u(\mathbf{x}) = 0, v(\mathbf{x}) = 0, \text{ and } w(\mathbf{x}) = w(x, y), \quad (1)$$



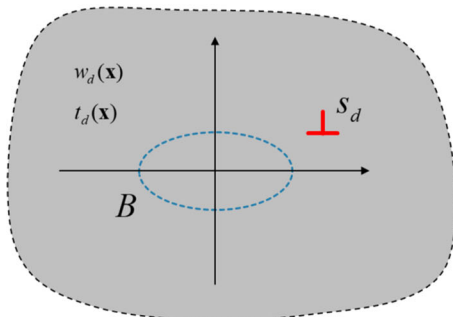
(a) An infinite-plane problem containing an elliptical inclusion subject to a screw dislocation



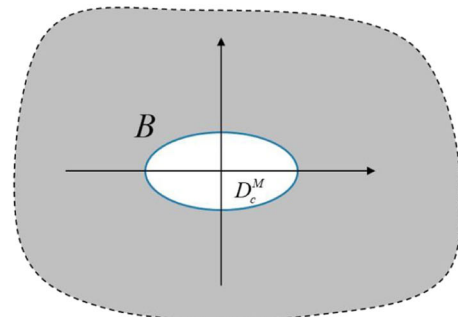
(b) An infinite matrix with an elliptical hole subject to a screw dislocation



(c) An interior Laplace problem for an elliptical inclusion (using the RBF)



(d) An infinite matrix subject to a screw dislocation (using the ABF)



(e) An exterior Laplace problem for the matrix (using the RBF)

FIG. 3. Sketch of an infinite plane with an elliptical inclusion subject to a screw dislocation by taking free body and using the superposition technique

where u and v are the vanishing components of displacement. The governing equation for the anti-plane displacement, w , in the absence of body force is simplified to

$$\nabla^2 w(\mathbf{x}) = 0, \mathbf{x} \in D, \tag{2}$$

where ∇^2 is the two-dimensional Laplace operator and D denotes the domain of interest. Therefore, the screw dislocation can be described as

$$\lim_{y \rightarrow y_d} (w(x, y^-) - w(x, y^+)) = b_z, x \geq x_d, \tag{3}$$

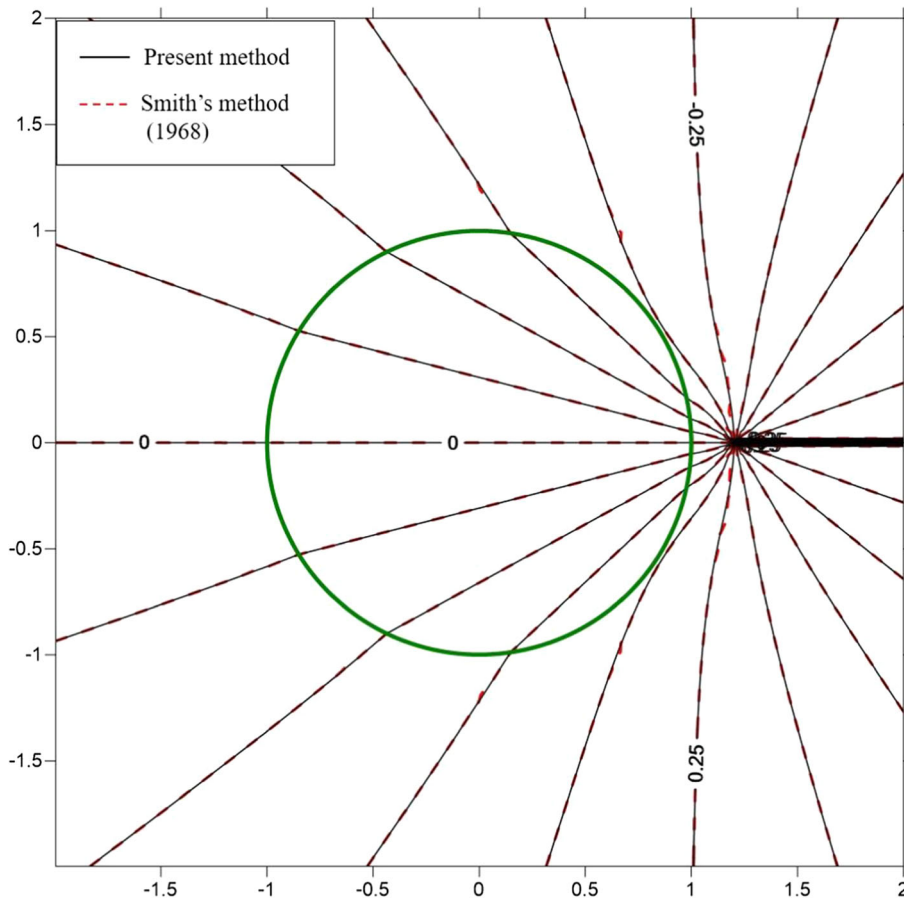


FIG. 4. Displacement contour of an infinite plane with a circular inclusion ($a = 1$, $b = 0.999$, $\mu^I = 0.6$ and $\mu^M = 1$)

where b_z denotes the component of the Burgers vector $(0, 0, b_z)$ along the anti-plane direction and (x_d, y_d) denotes the location of the screw dislocation. By taking the free body along the interface between the matrix and inclusion, the problem is decomposed into two systems. One is an infinite plane with an elliptical hole subject to a screw dislocation as shown in Fig. 3b. The other is that an elliptical inclusion bounded by the contour B which satisfies the Laplace equation as shown in Fig. 3c. For the problem in Fig. 3b, it can also be superimposed by two parts. One is a free field containing a screw dislocation and the other is an infinite plane with an elliptical hole, which satisfies the specified boundary condition as shown in Fig. 3d, e, respectively. The displacement and traction arising from the screw dislocation in Fig. 3d is expanded along the boundary by using the degenerate kernel and is introduced in the next section. In order to solve the interior and exterior typical boundary value problems (BVPs) in Fig. 3c, e, respectively, the null-field boundary integral formulation is reviewed and is elaborated on later. According to the displacement continuity and force equilibrium conditions on the interface between the matrix and inclusion, we have

$$w^M(\mathbf{x}) = w^I(\mathbf{x}), \mathbf{x} \in B, \quad (4)$$

$$\mu^M t^M(\mathbf{x}) = -\mu^I t^I(\mathbf{x}), \mathbf{x} \in B, \quad (5)$$

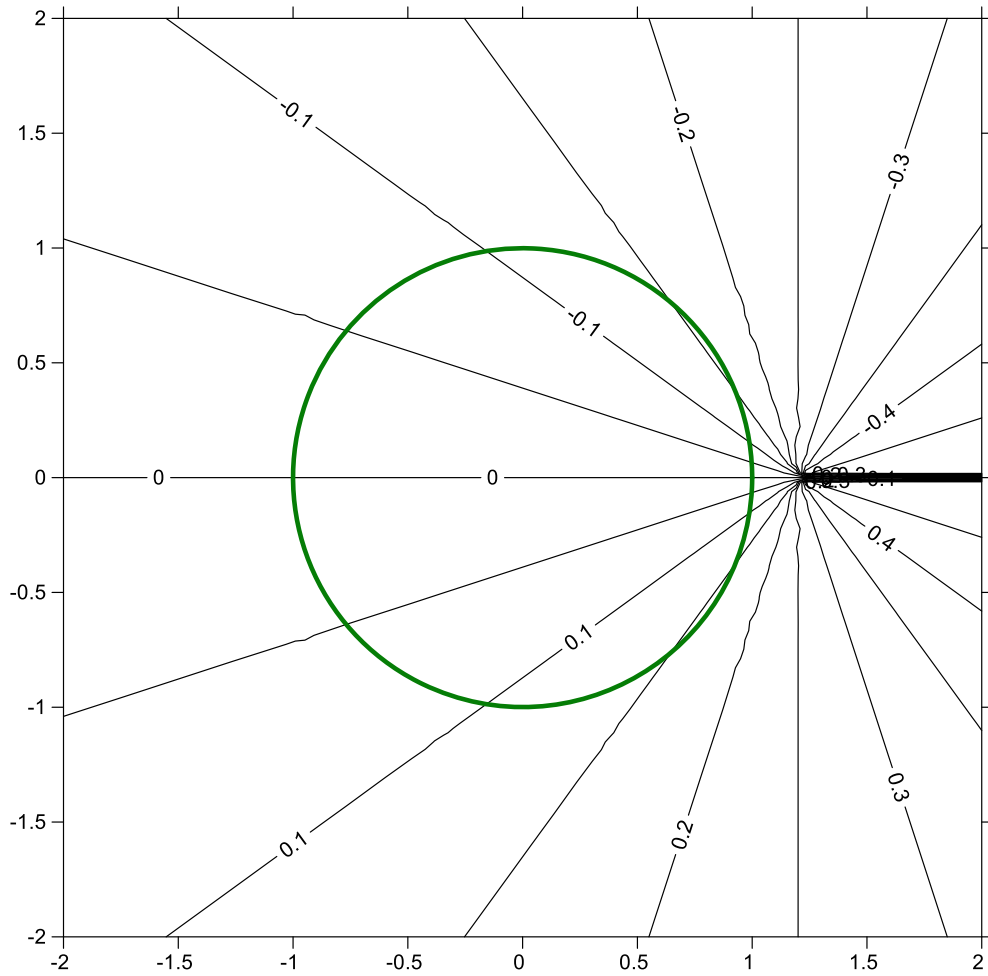


FIG. 5. Displacement contour of an infinite plane with a circular inclusion ($a = 1$, $b = 0.999$ and $\mu^I = \mu^M = 1$)

where μ^I and μ^M denote the shear moduli for the inclusion and matrix, respectively, and $t^{(\cdot)}(\mathbf{x}) = \partial w^{(\cdot)}(\mathbf{x})/\partial \mathbf{n}_x$ in which \mathbf{n}_x is the unit outward normal vector at \mathbf{x} .

3. Mathematical formulation

3.1. Transformation of the screw dislocation by using the degenerate kernel in the elliptical coordinates

In order to transform the screw dislocation with respect to the center of elliptical boundary, the degenerate kernel is used here. The kernel function in the elliptical coordinates is utilized to replace the Cartesian coordinates. Therefore, the location of the screw dislocation and collocation points are expressed as $\mathbf{s}_d = (\xi_d, \eta_d)$ and $\mathbf{x} = (\xi_x, \eta_x)$, respectively, in elliptical coordinates. In order to derive the degenerate kernel of screw dislocation of Laplace equation, we have

$$\ln(\mathbf{x} - \mathbf{s}_d) = \ln(re^{i\varphi}) = \ln r + i\varphi, \tag{6}$$

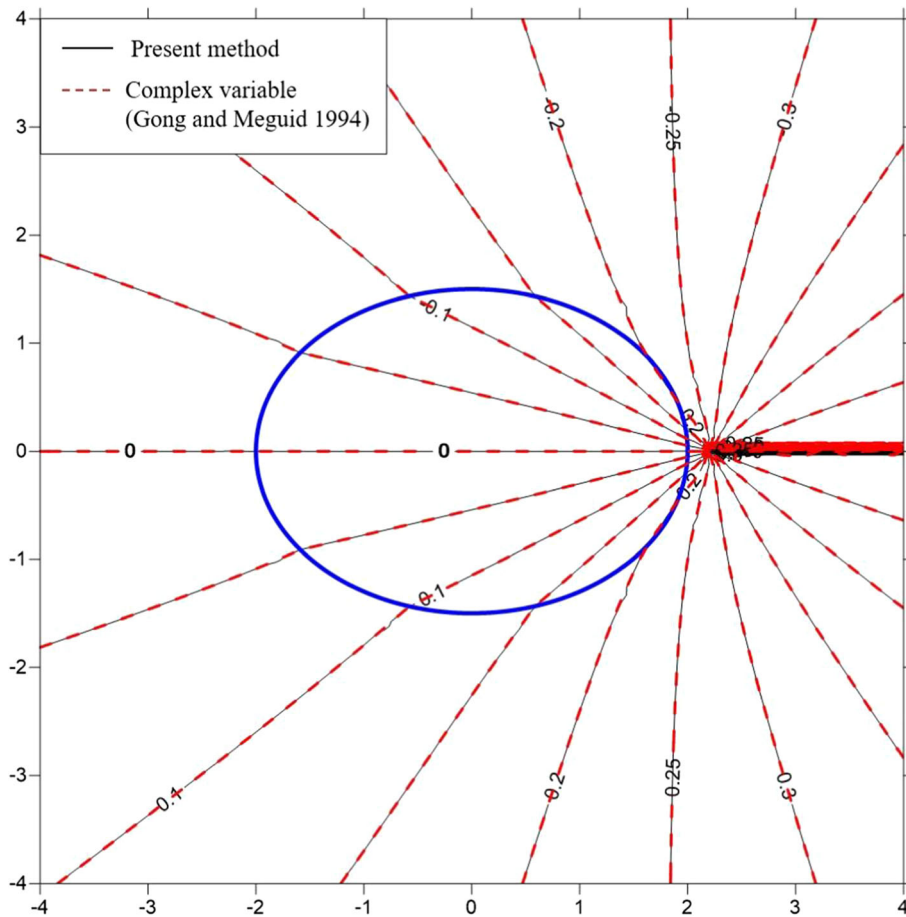


FIG. 6. Displacement contour of an infinite plane with an elliptical inclusion ($a = 2, b = 1.5, \mu^I = 0.6$ and $\mu^M = 1$)

where r and φ are the distance and argument, respectively, in the complex plane. For the exterior case ($\xi_d < \xi_x$), Eq. (6) can be expanded as follows:

$$\begin{aligned} \ln(\mathbf{x} - \mathbf{s}_d) = & \ln \frac{c}{2} + \xi_x - \sum_{m=1}^{\infty} \frac{1}{m} e^{-m(\xi_x + \xi_d)} \cos m(\eta_x + \eta_d) - \sum_{m=1}^{\infty} \frac{1}{m} e^{-m(\xi_x - \xi_d)} \cos m(\eta_x - \eta_d) \\ & + i\eta_x - \sum_{m=1}^{\infty} \frac{i}{m} e^{-m(\xi_x + \xi_d)} \sin m(\eta_x + \eta_d) - \sum_{m=1}^{\infty} \frac{i}{m} e^{-m(\xi_x - \xi_d)} \sin m(\eta_x - \eta_d), \quad \xi_d < \xi_x. \end{aligned} \quad (7)$$

It is interesting to find that the component in the degenerate kernel is nothing more than the complete Trefftz base. Thus, the degenerate (separable) form for the fundamental solution of the screw dislocation, $\varphi(\mathbf{s}_d, \mathbf{x})$, is obtained

$$\varphi(\mathbf{s}_d, \mathbf{x}) = \eta_x - \sum_{m=1}^{\infty} \frac{1}{m} e^{-m(\xi_x + \xi_d)} \sin m(\eta_x + \eta_d) - \sum_{m=1}^{\infty} \frac{1}{m} e^{-m(\xi_x - \xi_d)} \sin m(\eta_x - \eta_d), \quad \xi_d < \xi_x. \quad (8)$$

Similarly, we also obtain

$$\varphi(\mathbf{s}_d, \mathbf{x}) = \eta_d + \pi + \sum_{m=1}^{\infty} \frac{1}{m} e^{-m(\xi_x + \xi_d)} \sin m(\eta_x + \eta_d) + \sum_{m=1}^{\infty} \frac{1}{m} e^{-m(\xi_d - \xi_x)} \sin m(\eta_d - \eta_x), \quad \xi_d \geq \xi_x. \quad (9)$$

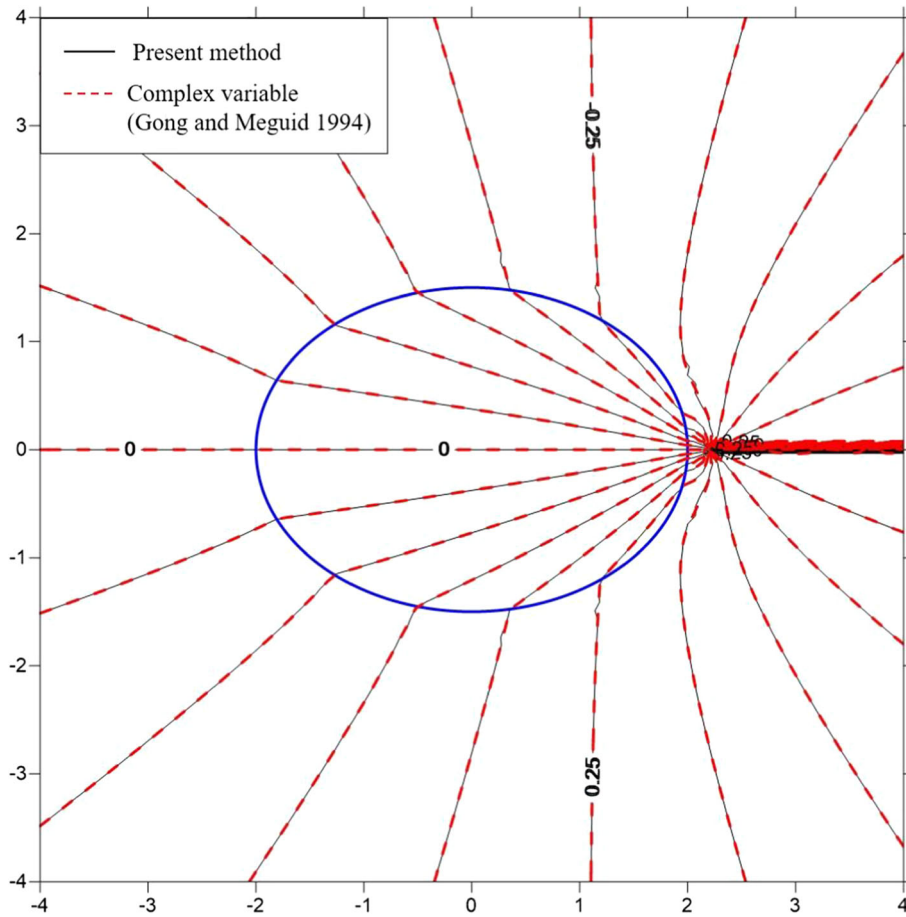


FIG. 7. Displacement contour of an infinite plane with an elliptical inclusion ($a = 2$, $b = 1.5$, $\mu^I = 0.2$ and $\mu^M = 1$)

for the interior case ($\xi_d \geq \xi_x$). The principal argument of angular basis function, $\varphi(\mathbf{s}_d, \mathbf{x})$ is defined in the interval between 0 and 2π . In order to match the physical meaning and mathematical requirement, we modify the range of the interest between $-\pi$ and π as shown in Table 1. Thus, the fundamental solution of the screw dislocation ($\varphi(\mathbf{s}_d, \mathbf{x})$) is expressed by

$$\varphi(\mathbf{s}_d, \mathbf{x}) = \begin{cases} \varphi^E(\xi_d, \eta_d; \xi_x, \eta_x) = \eta_x - \pi - \sum_{m=1}^{\infty} \frac{1}{m} e^{-m(\xi_x + \xi_d)} \sin m(\eta_x + \eta_d) \\ \quad - \sum_{m=1}^{\infty} \frac{1}{m} e^{-m(\xi_x - \xi_d)} \sin m(\eta_x - \eta_d), \quad \xi_d < \xi_x, \\ \varphi^I(\xi_d, \eta_d; \xi_x, \eta_x) = \eta_d + \sum_{m=1}^{\infty} \frac{1}{m} e^{-m(\xi_x + \xi_d)} \sin m(\eta_x + \eta_d) \\ \quad + \sum_{m=1}^{\infty} \frac{1}{m} e^{-m(\xi_d - \xi_x)} \sin m(\eta_d - \eta_x), \quad \xi_d \geq \xi_x, \end{cases} \quad (10)$$

where the superscripts “I” and “E” denote the interior and exterior cases, respectively. For the contour plot of the screw dislocation as shown in Table 1, the interior case means that the collocation point in the blue region and the exterior case means that the collocation point in the red region, where the screw dislocation is on the elliptical boundary.

TABLE 1. Degenerate kernels for the fundamental solution by using the RBF and the ABF

Polar coordinates	Re $[\ln(\mathbf{x} - \mathbf{s})]$ RBF [19]	$U(\mathbf{s}, \mathbf{x}) = \begin{cases} U^I(R, \theta; \rho, \phi) = \ln R - \sum_{m=1}^{\infty} \frac{1}{m} \left(\frac{\rho}{R}\right)^m \cos m(\theta - \phi), & R \geq \rho \\ U^E(R, \theta; \rho, \phi) = \ln \rho - \sum_{m=1}^{\infty} \frac{1}{m} \left(\frac{R}{\rho}\right)^m \cos m(\theta - \phi), & \rho > R \end{cases}$	
	Im $[\ln(\mathbf{x} - \mathbf{s})]$ ABF [25]	$\varphi(\mathbf{s}, \mathbf{x}) = \begin{cases} \varphi^I(R, \theta; \rho, \phi) = \theta + \sum_{m=1}^{\infty} \frac{1}{m} \left(\frac{\rho}{R}\right)^m \sin m(\theta - \phi), & R \geq \rho \\ \varphi^E(R, \theta; \rho, \phi) = \phi - \pi - \sum_{m=1}^{\infty} \frac{1}{m} \left(\frac{R}{\rho}\right)^m \sin m(\theta - \phi), & \rho > R \end{cases}$	
Elliptical coordinates	Re $[\ln(\mathbf{x} - \mathbf{s})]$ RBF [23]	$U(\mathbf{s}, \mathbf{x}) = \begin{cases} U^I(\xi_s, \eta_s; \xi_x, \eta_x) = \ln \frac{\xi}{2} + \xi_s - \sum_{m=1}^{\infty} \frac{1}{m} e^{-m(\xi_x + \xi_s)} \cos m(\eta_x) \\ \quad - \sum_{m=1}^{\infty} \frac{1}{m} e^{-m(\xi_s - \xi_x)} \cos m(\eta_s - \eta_x), & \xi_s \geq \xi_x \\ U^E(\xi_s, \eta_s; \xi_x, \eta_x) = \ln \frac{\xi}{2} + \xi_x \\ \quad - \sum_{m=1}^{\infty} \frac{1}{m} e^{-m(\xi_x + \xi_s)} \cos m(\eta_x + \eta_s) - \sum_{m=1}^{\infty} \frac{1}{m} e^{-m(\xi_x - \xi_s)} \cos m(\eta_x - \eta_s), & \xi_s < \xi_x \end{cases}$	
	Im $[\ln(\mathbf{x} - \mathbf{s})]$ ABF (Present result)	$\phi(\mathbf{s}, \mathbf{x}) = \begin{cases} \phi^I(\xi_s, \eta_s; \xi_x, \eta_x) = \eta_s + \sum_{m=1}^{\infty} \frac{1}{m} e^{-m(\xi_x + \xi_s)} \sin m(\eta_x + \eta_s) \\ \quad + \sum_{m=1}^{\infty} \frac{1}{m} e^{-m(\xi_s - \xi_x)} \sin m(\eta_s - \eta_x), & \xi_s \geq \xi_x \\ \phi^E(\xi_s, \eta_s; \xi_x, \eta_x) = \eta_x - \pi + \sum_{m=1}^{\infty} \frac{1}{m} e^{-m(\xi_x + \xi_s)} \sin m(\eta_x + \eta_s) \\ \quad + \sum_{m=1}^{\infty} \frac{1}{m} e^{-m(\xi_x - \xi_s)} \sin m(\eta_x - \eta_s), & \xi_s < \xi_x \end{cases}$	

3.2. Review of the null-field integral equations for the BVP

Following the success of the null-field boundary integral equation method for BVPs, a detailed formulation is reviewed here.

3.2.1. Null-field boundary integral formulation. By introducing the degenerate kernels, the collocation point can be located on the real boundary free of facing the principal value. Therefore, the integral representations of the exterior case including the boundary point can be written as

$$2\pi w(\mathbf{x}) = \int_B T^E(\mathbf{s}, \mathbf{x})w(\mathbf{s})dB(\mathbf{s}) - \int_B U^E(\mathbf{s}, \mathbf{x})\frac{\partial w(\mathbf{s})}{\partial \mathbf{n}_s}dB(\mathbf{s}), \quad \mathbf{x} \in D \cup B, \tag{11}$$

where \mathbf{s} and \mathbf{x} are the source and field points, respectively, B is the boundary, \mathbf{n}_x and \mathbf{n}_s denote the unit outward normal vector at the field point and the source point, respectively, and the kernel function $U(\mathbf{s}, \mathbf{x})$ is the fundamental solution $\ln r = \ln |\mathbf{x} - \mathbf{s}|$. The other kernel function can be obtained as $T(\mathbf{s}, \mathbf{x}) = \frac{\partial U(\mathbf{s}, \mathbf{x})}{\partial \mathbf{n}_s}$. The superscripts “ E ” of U and T kernels denote the corresponding degenerate kernel [23]. By moving the field point to the complementary domain, the null-field boundary integral equation is shown below:

$$0 = \int_B T^I(\mathbf{s}, \mathbf{x})w(\mathbf{s})dB(\mathbf{s}) - \int_B U^I(\mathbf{s}, \mathbf{x})\frac{\partial w(\mathbf{s})}{\partial \mathbf{n}_s}dB(\mathbf{s}), \quad \mathbf{x} \in D^c \cup B, \tag{12}$$

where D^c denotes the complementary domain of D .

3.2.2. Expansions of boundary densities by using the eigenfunction. To fully employ the property of elliptical geometry, the mathematical tools, degenerate kernel (so-called separable kernel) and eigenfunction expansion for an analytical study, the unknown boundary densities are represented by using the eigenfunction expansion as shown below:

$$w^M(\mathbf{s}) = \frac{b_z}{2\pi} \left(a_0^M + \sum_{n=1}^{\infty} a_n^M \cos n\eta_s + \sum_{n=1}^{\infty} b_n^M \sin n\eta_s \right), \tag{13}$$

$$w^I(\mathbf{s}) = \frac{b_z}{2\pi} \left(a_0^I + \sum_{n=1}^{\infty} a_n^I \cos n\eta_s + \sum_{n=1}^{\infty} b_n^I \sin n\eta_s \right), \tag{14}$$

$$\frac{\partial w^M(\mathbf{s})}{\partial \mathbf{n}_s} = t^M(\mathbf{s}) = \frac{1}{J_s} \frac{b_z}{2\pi} \left(p_0^M + \sum_{n=1}^{\infty} p_n^M \cos n\eta_s + \sum_{n=1}^{\infty} q_n^M \sin n\eta_s \right), \tag{15}$$

and

$$\frac{\partial w^I(\mathbf{s})}{\partial \mathbf{n}_s} = t^I(\mathbf{s}) = \frac{1}{J_s} \frac{b_z}{2\pi} \left(p_0^I + \sum_{n=1}^{\infty} p_n^I \cos n\eta_s + \sum_{n=1}^{\infty} q_n^I \sin n\eta_s \right), \tag{16}$$

where $J_s = c\sqrt{(\sinh \xi_s \cos \eta_s)^2 + (\cosh \xi_s \sin \eta_s)^2}$ and c is the half distance between the foci of the elliptical coordinates. In the elliptical coordinates, the boundary distribution of $w_d(\mathbf{x})$ and $\frac{\partial w_d(\mathbf{x})}{\partial \mathbf{n}_x} = -\frac{1}{J_x} \frac{\partial w_d(\mathbf{x})}{\partial \xi_x} = t_d(\mathbf{x})$ due to the screw dislocation are expressed as

$$w_d(\mathbf{x}) = \frac{b_z}{2\pi} \left(\eta_d + \sum_{m=1}^{\infty} \frac{1}{m} e^{-m(\xi_x + \xi_d)} \sin m(\eta_x + \eta_d) + \sum_{m=1}^{\infty} \frac{1}{m} e^{-m(\xi_d - \xi_x)} \sin m(\eta_d - \eta_x) \right),$$

$$\xi_x < \xi_d, \tag{17}$$

and

$$t_d(\mathbf{x}) = \frac{1}{J_x} \frac{b_z}{2\pi} \left(\sum_{m=1}^{\infty} e^{-m(\xi_x + \xi_d)} \sin m(\eta_x + \eta_d) - \sum_{m=1}^{\infty} e^{-m(\xi_d - \xi_x)} \sin m(\eta_d - \eta_x) \right), \quad \xi_x < \xi_d. \quad (18)$$

4. Illustrative examples and discussions

4.1. Revisit the problem of a screw dislocation by using the complex variables

Here, we focused on the interaction between a screw dislocation and an elliptical inhomogeneity. Smith [7] extended the circle theorem in hydrodynamics to derive the solution for the interaction between a screw dislocation and a circular inhomogeneity as shown below:

$$\begin{cases} F_M(z) = \frac{\mu^M b_z}{2\pi i} \left(\ln(z - z_0) + K \ln\left(\frac{R_0^2}{z} - \bar{z}_0\right) \right), \\ F_I(z) = (1 + K) \frac{\mu^M b_z}{2\pi i} \ln(z - z_0), \end{cases} \quad (19)$$

and

$$w(z) = \begin{cases} \frac{1}{\mu^M} \operatorname{Re} [F_M(z)], & \text{for the matrix,} \\ \frac{1}{\mu^I} \operatorname{Re} [F_I(z)], & \text{for the inclusion,} \end{cases} \quad (20)$$

where $K = (\mu^I - \mu^M) / (\mu^I + \mu^M)$, z_0 is the location of a screw dislocation outside the circular inclusion, R_0 is the radius of the circle, and $F_M(z)$ and $F_I(z)$ are potential functions in the matrix and the inhomogeneity, respectively. For an elliptical inclusion with semi-major and semi-minor axes a and b , he introduced the conformal mapping as shown below:

$$\begin{aligned} z &= f(z_1) = \frac{R_0}{a+b} \left(z_1 + (z_1^2 - c^2)^{1/2} \right), \\ z_1 &= g(z) = \frac{c}{2} \left(kz + \frac{1}{kz} \right), \end{aligned} \quad (21)$$

where c is the half distance between the foci and $k = \frac{\sqrt{a+b}}{\sqrt{a-b}}$. However, the ellipse in the z_1 plane is mapped to concentric circles instead of a circle as shown in Fig. 1. The radii of outer and inner circles are R_0 and R_1 , respectively. Sendekyj [1] employed the mapping function to obtain the potential function as given below:

$$\begin{aligned} F_M(g(z)) &= \frac{\mu^M b_z}{2\pi i} \left(\ln(z - z_0) + K \ln\left(z - \frac{1}{z_0}\right) + \ln\left(z - \frac{\lambda}{z_0}\right) \right. \\ &\quad \left. + K \ln\left(z - \frac{z_0}{\lambda}\right) - (1 + K) \ln z + \ln c + K \ln cz \right), \end{aligned} \quad (22)$$

where $\lambda = R_1^2 = \frac{a-b}{a+b}$. It meant that $F_M(z)$ in Eq. (22) consists the rigid body term, $\ln c$ and five screw dislocations in the z plane as shown in Fig. 2. It violates the condition of a dislocation only at z_0 . Sendekyj introduced the corresponding dislocations to eliminate the extra dislocations in the z plane [1]. He derived an alternative expression for $F_M(z_1)$ as shown below:

$$\begin{aligned} F_M(g(z)) &= \frac{\mu^M b_z}{2\pi i} \left\{ \ln(z - z_0) + K \left(\ln\left(z - \frac{1}{z_0}\right) - \ln z \right) \right. \\ &\quad \left. + (1 - K^2) \sum_{n=0}^{\infty} (-K)^n \left(\ln\left(z - \frac{\lambda^{n+1}}{z_0}\right) - \ln z \right) \right\}. \end{aligned} \quad (23)$$

The solution for screw dislocation near a circular boundary is in agreement of Smith [7] and Dundurs [35]. But the expression for the inclusion, $F_I(z)$ was not proposed in [1]. Until 1994, Gong and Meguid revisited this problem [2]. They used the Laurent series to represent the potential. In addition to the

interface conditions in Eqs. (4) and (5) for B_0 , an extra condition must be satisfied on B_1 as shown below:

$$F_I(z) = F_I(\bar{z}), \quad z \in B_1. \tag{24}$$

The alternative expression for $F_M(z_1)$ was derived as shown below:

$$F_M(g(z)) = \frac{\mu^M b_z}{2\pi i} \left\{ \ln(z - z_0) - \sum_{m=1}^{\infty} \frac{K\lambda^{-m}}{K + \lambda^{-m}} \frac{1}{m + 1} (zz_0)^{-m} \right\}. \tag{25}$$

The potential in the inclusion was

$$F_I(g(z)) = \sum_{n=0}^{\infty} c_n z^{n+1} + d_n z^{-(n+1)}, \tag{26}$$

where coefficients are

$$c_n = L_n \bar{a}_n + N_n a_n, \text{ and } d_n = \lambda^{n+1} (L_n \bar{a}_n + N_n a_n),$$

in which

$$L_n = K(1 + K)\lambda^{-(n+1)}/\Delta, \quad N_n = (1 + K)\lambda^{-2(n+1)}/\Delta, \quad a_n = -\frac{\mu^M b_z}{2\pi i} \frac{1}{n + 1} z_0^{-(n+1)}, \tag{27}$$

$$\text{and } \Delta = \lambda^{-2(n+1)} - K^2.$$

To verify the equivalence between Eqs. (23) and (25), Eq. (23) could be expanded as

$$F_M(g(z)) = \frac{\mu^M b_z}{2\pi i} \left\{ \ln(z - z_0) - K \sum_{m=1}^{\infty} \frac{1}{m} (zz_0)^{-m} - (1 - K^2) \sum_{n=0}^{\infty} (-K)^n \sum_{m=1}^{\infty} \frac{1}{m} (zz_0)^{-m} \lambda^{m(n+1)} \right\}. \tag{28}$$

By taking the Taylor series for series terms in Eq. (25), we have

$$F_M(g(z)) = \frac{\mu^M b_z}{2\pi i} \left\{ \ln(z - z_0) - K \sum_{m=1}^{\infty} \frac{1}{m} (zz_0)^{-m} + K^2 \sum_{m=1}^{\infty} \frac{1}{m} (zz_0)^{-m} \sum_{n=0}^{\infty} (-K)^n \lambda^{m(n+1)} \right\}. \tag{29}$$

Unfortunately, the result of Eqs. (28) and (29) does not match in our plot, i.e., the error may exist. The above three methods by Smith [7], Sendecyk [1], Gong and Meguid [2] were compared in Table 2. It is why we revisit this issue by using the alternative and independent approach, the angular basis function. This method is free of the extra dislocations or modification to match the boundary condition. Some numerical results verified the results.

4.2. The present method—degenerate kernel of the angular basis function

By employing the superposition technique, an anti-plane problem with a screw dislocation is decomposed into two parts. One is the infinite plane subject to the screw dislocation, and the other is the infinite plane with an elliptical inhomogeneity subject to the corresponding B.C. For the inclusion, the null-field boundary integral equation is rewritten as

$$0 = \int_B T^E(\mathbf{s}, \mathbf{x}) w^I(\mathbf{s}) dB(\mathbf{s}) - \int_B U^E(\mathbf{s}, \mathbf{x}) t^I(\mathbf{s}) dB(\mathbf{s}), \quad \mathbf{x} \in D_c^I \cup B, \tag{30}$$

TABLE 2. Comparison of three approaches to deal with the elliptical inclusion in the complex variables

Method	Smith [7]	Sendeckyj [1]	Gong and Meguid [2]
Key technique	Conformal mapping	Image method	Laurent series
Extra operation	N.A.	Corresponding dislocations to eliminate the extra dislocations	Extra B.C. $F_I(z) = F_I(\bar{z}), z \in B_1$
The potential in the matrix	$F_M(g(z)) = \frac{\mu^M b_z}{2\pi i} \ln(z - z_0) + \frac{\mu^M b_z}{2\pi i} \ln\left(\frac{R_0^2}{z} - \bar{z}_0\right)$	$F_M(g(z)) = \frac{\mu^M b_z}{2\pi i} \left\{ \ln(z - z_0) + K \left(\ln\left(z - \frac{1}{z_0}\right) - \ln z \right) + (1 - K^2) \sum_{n=0}^{\infty} (-K)^n \left(\ln\left(z - \frac{\lambda^{n+1}}{z_0}\right) - \ln z \right) \right\}$	$F_M(g(z)) = \frac{\mu^M b_z}{2\pi i} \left\{ - \sum_{m=1}^{\infty} \frac{K \lambda^{-m}}{K + \lambda^{-m}} \frac{1}{m+1} (zz_0)^{-m} \right\}$
The potential in the inclusion	N.A.	N.A.	$F_I(g(z)) = \frac{\mu^M b_z}{2\pi i} \left\{ - \sum_{m=1}^{\infty} \frac{K \lambda^{-m-1}}{K + \lambda^{-m-1}} \frac{1}{m+1} (zz_0)^{-m} \right\} = \sum_{n=0}^{\infty} c_n z^{n+1} + d_n z^{-(n+1)},$ $c_n = L_n \bar{a}_n + N_n a_n,$ $d_n = \lambda^{n+1} (L_n \bar{a}_n + N_n a_n),$ $L_n = K(1 + K) \lambda^{-(n+1)} / \Delta,$ $N_n = (1 + K) \lambda^{-2(n+1)} / \Delta,$ $a_n = -\frac{\mu^M b_z}{2\pi i} \frac{1}{n+1} z_0^{-(n+1)},$ and $\Delta = \lambda^{-2(n+1)} - K^2$

where we adopt the degenerate kernel to represent $\ln r$ instead of φ , D_c^I is the complementary domain of an elliptical inclusion as shown in Fig. 3c,

$$U(\mathbf{s}, \mathbf{x}) = \begin{cases} U^E(\mathbf{s}, \mathbf{x}) = \ln \frac{c}{2} + \xi_{\mathbf{x}} - \sum_{m=1}^{\infty} \frac{1}{m} e^{-m(\xi_{\mathbf{x}} + \xi_{\mathbf{s}})} \cos m(\eta_{\mathbf{x}} + \eta_{\mathbf{s}}) \\ \quad - \sum_{m=1}^{\infty} \frac{1}{m} e^{-m(\xi_{\mathbf{x}} - \xi_{\mathbf{s}})} \cos m(\eta_{\mathbf{x}} - \eta_{\mathbf{s}}), \xi_{\mathbf{x}} \geq \xi_{\mathbf{s}}, \\ U^I(\mathbf{s}, \mathbf{x}) = \ln \frac{c}{2} + \xi_{\mathbf{s}} - \sum_{m=1}^{\infty} \frac{1}{m} e^{-m(\xi_{\mathbf{x}} + \xi_{\mathbf{s}})} \cos m(\eta_{\mathbf{x}} + \eta_{\mathbf{s}}) \\ \quad - \sum_{m=1}^{\infty} \frac{1}{m} e^{-m(\xi_{\mathbf{s}} - \xi_{\mathbf{x}})} \cos m(\eta_{\mathbf{s}} - \eta_{\mathbf{x}}), \xi_{\mathbf{x}} < \xi_{\mathbf{s}}, \end{cases} \quad (31)$$

and

$$T(\mathbf{s}, \mathbf{x}) = \begin{cases} T^E(\mathbf{s}, \mathbf{x}) = \frac{1}{J_{\mathbf{s}}} \left(\sum_{m=1}^{\infty} e^{-m(\xi_{\mathbf{x}} + \xi_{\mathbf{s}})} \cos m(\eta_{\mathbf{x}} + \eta_{\mathbf{s}}) \right. \\ \quad \left. - \sum_{m=1}^{\infty} e^{-m(\xi_{\mathbf{x}} - \xi_{\mathbf{s}})} \cos m(\eta_{\mathbf{x}} - \eta_{\mathbf{s}}) \right), \xi_{\mathbf{x}} > \xi_{\mathbf{s}}, \\ T^I(\mathbf{s}, \mathbf{x}) = \frac{1}{J_{\mathbf{s}}} \left(1 + \sum_{m=1}^{\infty} e^{-m(\xi_{\mathbf{x}} + \xi_{\mathbf{s}})} \cos m(\eta_{\mathbf{x}} + \eta_{\mathbf{s}}) \right. \\ \quad \left. + \sum_{m=1}^{\infty} e^{-m(\xi_{\mathbf{s}} - \xi_{\mathbf{x}})} \cos m(\eta_{\mathbf{x}} - \eta_{\mathbf{s}}) \right), \xi_{\mathbf{x}} < \xi_{\mathbf{s}}. \end{cases} \quad (32)$$

After substituting Eqs. (14), (16), (31) and (32) into Eq. (30) and collocating the field point \mathbf{x} on the boundary, we have

$$\begin{aligned} & \sum_{n=1}^{\infty} \pi e^{-2n\xi_0} (a_n^I \cos n\eta_{\mathbf{x}} - b_n^I \sin n\eta_{\mathbf{x}}) - \sum_{n=1}^{\infty} \pi (a_n^I \cos n\eta_{\mathbf{x}} + b_n^I \sin n\eta_{\mathbf{x}}) \\ &= 2\pi \left(\ln \frac{c}{2} + \xi_0 \right) p_0^I \\ & \quad - \sum_{n=1}^{\infty} \frac{\pi}{n} e^{-2n\xi_0} (p_n^I \cos n\eta_{\mathbf{x}} - q_n^I \sin n\eta_{\mathbf{x}}) - \sum_{n=1}^{\infty} \frac{\pi}{n} (p_n^I \cos n\eta_{\mathbf{x}} + q_n^I \sin n\eta_{\mathbf{x}}), \end{aligned} \quad (33)$$

where ξ_0 is the radial parameter in the elliptical coordinates for the interface. By comparing with the coefficients of Fourier base in Eq. (33), we have

$$\begin{cases} p_0^I = 0, \\ a_n^I = -\frac{1}{n} \left(\frac{e^{-2n\xi_0} + 1}{e^{-2n\xi_0} - 1} \right) p_n^I, n = 1, 2, \dots, \\ b_n^I = -\frac{1}{n} \left(\frac{e^{-2n\xi_0} - 1}{e^{-2n\xi_0} + 1} \right) q_n^I, n = 1, 2, \dots, \end{cases} \quad (34)$$

By satisfying the continuity condition on the interface of Eqs. (4) and (5), we obtained

$$\begin{cases} p_0^M = -\frac{\mu^I}{\mu^M} p_0^I = 0, \\ p_n^M = -\frac{\mu^I}{\mu^M} p_n^I, n = 1, 2, \dots, \\ q_n^M = -\frac{\mu^I}{\mu^M} q_n^I, n = 1, 2, \dots, \end{cases} \quad (35)$$

and

$$\begin{cases} a_0^M = a_0^I, \\ a_n^M = a_n^I = \frac{1}{n} \frac{\mu^M}{\mu^I} \left(\frac{e^{-2n\xi_0} + 1}{e^{-2n\xi_0} - 1} \right) p_n^M, n = 1, 2, \dots, \\ b_n^M = b_n^I = \frac{1}{n} \frac{\mu^M}{\mu^I} \left(\frac{e^{-2n\xi_0} - 1}{e^{-2n\xi_0} + 1} \right) q_n^M, n = 1, 2, \dots. \end{cases} \quad (36)$$

According to the superposition technique and the null-field boundary integral equation, we have

$$0 = \int_B T^I(\mathbf{s}, \mathbf{x}) (w^M(\mathbf{s}) - w_d(\mathbf{s})) dB(\mathbf{s}) - \int_B U^I(\mathbf{s}, \mathbf{x}) (t^M(\mathbf{s}) - t_d(\mathbf{s})) dB(\mathbf{s}), \quad \mathbf{x} \in D_c^M \cup B, \quad (37)$$

where D_c^M is the complementary domain of the matrix as shown in Fig. 3e,

$$w_d(\mathbf{s}) = \frac{b_z}{2\pi} \left(\eta_d + \sum_{m=1}^{\infty} \frac{1}{m} e^{-m(\xi_0 + \xi_d)} \sin m(\eta_s + \eta_d) + \sum_{m=1}^{\infty} \frac{1}{m} e^{-m(\xi_d - \xi_0)} \sin m(\eta_d - \eta_s) \right),$$

$$\mathbf{s} = (\xi_0, \eta_s) \in B \quad (38)$$

and

$$t_d(\mathbf{s}) = \frac{1}{J_s} \frac{b_z}{2\pi} \left(\sum_{m=1}^{\infty} e^{-m(\xi_0 + \xi_d)} \sin m(\eta_s + \eta_d) - \sum_{m=1}^{\infty} e^{-m(\xi_d - \xi_0)} \sin m(\eta_d - \eta_s) \right), \quad \mathbf{s} = (\xi_0, \eta_s) \in B. \quad (39)$$

After substituting Eqs. (31), (32), (34)–(36), (38) and (39) into Eq. (37) and collocating the field point \mathbf{x} on the boundary, Eq. (37) yields

$$\begin{aligned} & - \left(2\pi\eta_d + \sum_{m=1}^{\infty} \frac{2\pi}{m} e^{-m(\xi_d - \xi_0)} \sin m(\eta_d - \eta_x) + \sum_{m=1}^{\infty} \frac{2\pi}{m} e^{-m(\xi_d + \xi_0)} \sin m(\eta_d + \eta_x) \right) \\ & = - \left(2\pi a_0^M + \sum_{n=1}^{\infty} \frac{\pi}{n} (e^{-2n\xi_0} + 1) \left(\frac{\mu^M}{\mu^I} \left(\frac{e^{-2n\xi_0} + 1}{e^{-2n\xi_0} - 1} \right) - 1 \right) p_n^M \cos n\eta_x \right. \\ & \quad \left. - \sum_{n=1}^{\infty} \frac{\pi}{n} (e^{-2n\xi_0} - 1) \left(\frac{\mu^M}{\mu^I} \left(\frac{e^{-2n\xi_0} - 1}{e^{-2n\xi_0} + 1} \right) - 1 \right) q_n^M \sin n\eta_x \right). \end{aligned} \quad (40)$$

By comparing with the coefficient of the Fourier sine base in Eq. (40), we have

$$\begin{cases} p_0^I = 0, \\ a_n^I = -\frac{1}{n} \left(\frac{e^{-2n\xi_0} + 1}{e^{-2n\xi_0} - 1} \right) p_n^I, \quad n = 1, 2, \dots, \\ b_n^I = -\frac{1}{n} \left(\frac{e^{-2n\xi_0} - 1}{e^{-2n\xi_0} + 1} \right) q_n^I, \quad n = 1, 2, \dots, \end{cases} \quad (41)$$

Based on Eqs. (34), (35), (36) and (41), the unknown Fourier coefficients could be determined by

$$\begin{cases} a_0^I = a_0^M = \eta_d, \\ a_n^I = a_n^M = \frac{2}{n} \frac{\mu^M (e^{-n(\xi_d + \xi_0)} + e^{-n(\xi_d - \xi_0)})}{(\mu^M - \mu^I) e^{-2n\xi_0} + (\mu^M + \mu^I)} \sin n\eta_d, \quad n = 1, 2, \dots, \\ b_n^I = b_n^M = -\frac{2}{n} \frac{\mu^M (e^{-n(\xi_d + \xi_0)} - e^{-n(\xi_d - \xi_0)})}{(\mu^M - \mu^I) e^{-2n\xi_0} - (\mu^M + \mu^I)} \cos n\eta_d, \quad n = 1, 2, \dots \end{cases} \quad (42)$$

Finally, the analytical solution derived by the present method is given below. For the matrix, we have

$$w(\mathbf{x}) = w^M(\mathbf{x}) = \begin{cases} \frac{b_z}{2\pi} \left(\eta_x - \pi + \sum_{n=1}^{\infty} \frac{1}{n} e^{-n(\xi_x - \xi_d)} \sin n(\eta_x - \eta_d) \right. \\ \quad \left. + \sum_{n=1}^{\infty} \frac{1}{n} e^{-n(\xi_x + \xi_d - 2\xi_0)} \frac{\mu^M (e^{-2n\xi_0} + 1) + \mu^I (e^{-2n\xi_0} - 1)}{\mu^M (e^{-2n\xi_0} + 1) - \mu^I (e^{-2n\xi_0} - 1)} \sin n\eta_d \cos n\eta_x \right. \\ \quad \left. - \sum_{n=1}^{\infty} \frac{1}{n} e^{-n(\xi_x + \xi_d - 2\xi_0)} \frac{\mu^M (e^{-2n\xi_0} - 1) + \mu^I (e^{-2n\xi_0} + 1)}{\mu^M (e^{-2n\xi_0} - 1) - \mu^I (e^{-2n\xi_0} + 1)} \cos n\eta_d \sin n\eta_x \right), \quad \xi_x \geq \xi_d, \\ \frac{b_z}{2\pi} \left(\eta_d + \sum_{n=1}^{\infty} \frac{1}{n} e^{-n(\xi_d - \xi_x)} \sin n(\eta_d - \eta_x) \right. \\ \quad \left. + \sum_{n=1}^{\infty} \frac{1}{n} e^{-n(\xi_x + \xi_d - 2\xi_0)} \frac{\mu^M (e^{-2n\xi_0} + 1) + \mu^I (e^{-2n\xi_0} - 1)}{\mu^M (e^{-2n\xi_0} + 1) - \mu^I (e^{-2n\xi_0} - 1)} \sin n\eta_d \cos n\eta_x \right. \\ \quad \left. - \sum_{n=1}^{\infty} \frac{1}{n} e^{-n(\xi_x + \xi_d - 2\xi_0)} \frac{\mu^M (e^{-2n\xi_0} - 1) + \mu^I (e^{-2n\xi_0} + 1)}{\mu^M (e^{-2n\xi_0} - 1) - \mu^I (e^{-2n\xi_0} + 1)} \cos n\eta_d \cos n\eta_x \right), \quad \xi_0 \leq \xi_x < \xi_d. \end{cases} \quad (43)$$

For the inclusion, we have

$$w(\mathbf{x}) = w^I(\mathbf{x}) = \frac{b_z}{2\pi} \left(\eta_d + \sum_{n=1}^{\infty} \frac{2}{n} \frac{\mu^M (e^{-n(\xi_d + \xi_{\mathbf{x}})} + e^{-n(\xi_d - \xi_{\mathbf{x}})})}{(\mu^M - \mu^I)e^{-2n\xi_0} + (\mu^M + \mu^I)} \sin n\eta_d \cos n\eta_{\mathbf{x}} - \sum_{n=1}^{\infty} \frac{2}{n} \frac{\mu^M (e^{-n(\xi_d + \xi_{\mathbf{x}})} - e^{-n(\xi_d - \xi_{\mathbf{x}})})}{(\mu^M - \mu^I)e^{-2n\xi_0} - (\mu^M + \mu^I)} \cos n\eta_d \sin n\eta_{\mathbf{x}} \right), \quad \xi_{\mathbf{x}} < \xi_0. \tag{44}$$

First, a special case, a circular inclusion in the infinite plane with a screw dislocation is examined. In the literature [7], an analytical solution of the circular case was derived by Smith as shown in Eqs. (19) and (20). The screw dislocation is located at $\mathbf{s}_d = (1.2, 0)$. For the present method, the center of the elliptical inclusion is set at $(0, 0)$. The semimajor and semiminor axes of the ellipse, $a = 1$ and $b = 0.999$, respectively, are selected to simulate a circular case. The shear moduli for the inclusion and matrix are $\mu^I = 0.6$ and $\mu^M = 1$, respectively. Figure 4 shows the displacement contour by using the Smith’s method [7] and the present method. It is found that the result of the present approach matches well with that of using the Smith’s method. Besides, the special case, $\mu^I = \mu^M = 1$, is also addressed in Fig. 5.

For an elliptical case, the screw dislocation is located at $\mathbf{s}_d = (2.2, 0)$. The center of the elliptical inclusion is set at $(0, 0)$. The semimajor and semiminor axes of the ellipse are $a = 2$ and $b = 1.5$, respectively. The shear moduli for the inclusion and matrix are $\mu^I = 0.6$ and $\mu^M = 1$, respectively. By comparing with the results of ours and the literatures [1, 2], we find a typo in Eq. (25) which was derived by Gong and Meguid [2]. Equation (25) should be corrected as

$$F_M(g(z)) = \frac{\mu^M b_z}{2\pi i} \left\{ \ln(z - z_0) - \sum_{m=1}^{\infty} \frac{K\lambda^{-m} - 1}{K + \lambda^{-m}} \frac{1}{m + 1} (zz_0)^{-m} \right\}. \tag{45}$$

Therefore, the equivalence between Eqs. (23) and (45) can be proved by expanding Eq. (23) into the Taylor series for series terms in Eq. (45). Figure 6 shows the displacement contour by using the Gong and Meguid’s method [2] and the present method. By correcting the new representation formula in Eq. (45) instead of Eq. (25), their results agree well with ours. While the shear moduli for the inclusion and matrix are $\mu^I = 0.2$ and $\mu^M = 1$, respectively, the agreeable results are also obtained as shown in Fig. 7.

5. Conclusions

Following the previous successful experience of a circular case, the infinite plane problem containing an elliptical inhomogeneity subject to the screw dislocation was analytically solved here. The degenerate kernel and superposition technique were employed to solve the BVP. Moreover, the angle-type fundamental solution for the screw dislocation in terms of degenerate kernel for polar coordinates was extended to the elliptical coordinates in this paper. By using the ABF, the boundary displacement and traction caused by the screw dislocation along the elliptical interface can be obtained. The interaction between a screw dislocation and an elliptical inhomogeneity was investigated to show the validity of the present method. Besides, one limiting case of a circular inclusion by approaching the length of the axes was also addressed for comparison. Finally, good agreements were made after comparing with those of complex variables. The expression of Gong and Meguid’s solution was also corrected. Although the result of complex variables can extend to other domains by using the conformal mapping, the extra boundary condition may be considered like this case. The present approach can extend to other shapes by using the suitable degenerate kernel, even the three-dimensional case. In addition, it is also possible to extend multiple inclusions by using this method combining with the adaptive observer.

Acknowledgements

Financial supports from the Ministry of Science and Technology under Grant No. MOST-108-2221-E-019-048 for National Taiwan Ocean University are gratefully acknowledged.

Publisher's Note Springer Nature remains neutral with regard to jurisdictional claims in published maps and institutional affiliations.

Springer Nature or its licensor holds exclusive rights to this article under a publishing agreement with the author(s) or other rightsholder(s); author self-archiving of the accepted manuscript version of this article is solely governed by the terms of such publishing agreement and applicable law.

References

- [1] Sendekyj, G.P.: Screw dislocation in inhomogeneous solids. In: Simmons, J.A., et al. (eds.) *Fundamental Aspects of Dislocation Theory*, pp. 57–69. US National Bureau of Standards, Gaithersburg (1970)
- [2] Gong, S.X., Meguid, S.A.: A screw dislocation interacting with an elastic elliptical inhomogeneity. I. *Int. J. Eng. Sci.* **32**(8), 1221–1228 (1994)
- [3] Head, A.K.: The interaction of dislocations and boundaries. *Phil. Mag. Ser. 7* **44**, 92–94 (1953)
- [4] Head, A.K.: Edge dislocations in inhomogeneous media. *Proc. Phys. Soc. B* **66**, 793–801 (1953)
- [5] Chen, F.M., Chao, C.K., Chen, C.K.: Interaction of an edge dislocation with a coated elliptic inclusion. *Int. J. Solids Struct.* **48**(10), 1451–1465 (2011)
- [6] Zhou, K., Hoh, H.J., Wang, X., Keer, L.M., Pang, J.H.L., Song, B., Wang, Q.J.: A review of recent works on inclusions. *Mech. Mater.* **60**, 144–158 (2013)
- [7] Smith, E.: The interaction between dislocations and inhomogeneities. I. *Int. J. Eng. Sci.* **6**, 129–143 (1968)
- [8] Shen, M.-H.: A magnetoelectric screw dislocation interacting with a circular layered inclusion. *Eur. J. Mech. A-Solids* **27**, 429–442 (2008)
- [9] Wang, X., Pan, E., Roy, A.K.: Interaction between a screw dislocation and a piezoelectric circular inclusion with viscous interface. *J. Mech. Mater. Struct.* **3**, 761–773 (2008)
- [10] Ang, W.T., Kang, I.: A complex variable boundary element method for elliptic partial differential equations in a multiply connected region. *Int. J. Comput. Math.* **75**, 515–525 (2000)
- [11] Chen, Y.Z., Lin, X.Y.: Solutions of the interior and exterior boundary value problems in plane elasticity by using dislocation distribution layer. *Int. J. Solids Struct.* **47**, 355–364 (2010)
- [12] Sendekyj, G.P.: Screw dislocations near circular inclusions. *Phys. Stat. Sol.* **3**, 529–535 (1970)
- [13] Fang, Q., Liu, Y., Jiang, P.: Interaction between a screw dislocation and an elastic elliptical inhomogeneity with interfacial cracks. *Acta. Mech. Sin.* **21**, 151–159 (2005)
- [14] Luo, J., Xiao, Z.M.: Analysis of a screw dislocation interacting with an elliptical nano inhomogeneity. *Int. J. Eng. Sci.* **47**, 883–893 (2009)
- [15] Wang, X., Schiavone, P.: A screw dislocation near a semi-infinite crack partially penetrating an elastic inhomogeneity of arbitrary shape. *Acta Mech.* **232**, 2919–2931 (2021)
- [16] Lubarda, V.A.: Dislocation Burgers vector and the Peach–Koehler force: a review. *J. Mater. Res. Technol.* **8**(1), 1550–1565 (2019)
- [17] Kansa, E.J.: Multiquadrics-A scattered data approximation scheme with applications to computational fluid-dynamics-II solutions to parabolic, hyperbolic and elliptic partial differential equations. *Comput. Math. Appl.* **19**(8–9), 147–161 (1990)
- [18] Zheng, H., Zhang, Ch., Wang, Y., Sladek, J., Sladek, V.: A meshfree local RBF collocation method for anti-plane transverse elastic wave propagation analysis in 2D phononic crystals. *J. Comput. Phys.* **305**, 997–1014 (2016)
- [19] Chen, J.T., Chiu, Y.P.: On the pseudo-differential operators in the dual boundary integral equations using degenerate kernels and circulants. *Eng. Anal. Bound. Elem.* **26**, 41–35 (2002)
- [20] Chen, J.T., Chou, K.H., Kao, S.K.: Derivation of Green's function using addition theorem. *Mech. Res. Commun.* **36**(3), 351–363 (2009)
- [21] Chen, J.T., Kao, J.H., Huang, Y.L., Kao, S.K.: On the stress concentration factor of circular/elliptic hole and rigid inclusion under the remote anti-plane shear by using degenerate kernels. *Arch. Appl. Mech.* **91**, 1133–1155 (2021)
- [22] Chen, J.T., Kao, J.H., Huang, Y.L.: Study on the stress intensity factor and the double-degeneracy mechanism in the BEM/BIEM for anti-plane shear problems. *Theor. Appl. Fract. Mech.* **112**, 102830 (2021)
- [23] Morse, P.M., Feshbach, H.: *Methods of Theoretical Physics*. McGraw-Hill, New York (1978)

- [24] Golberg, M.A.: *Solution Methods for Integral Equations: Theory and Applications*. Plenum Press, New York (1979)
- [25] Chen, J.T., Chou, K.H., Lee, Y.T.: A novel method for solving the displacement and stress fields of an infinite domain with circular holes and/or inclusions subject to a screw dislocation. *Acta Mech.* **218**, 115–132 (2011)
- [26] Young, D.L., Huang, Y.J., Wu, C.S., Sladek, V., Sladek, J.: Angular-basis functions formulation for 2D potential flows with non-smooth boundaries. *Eng. Anal. Bound. Elem.* **61**, 1–15 (2015)
- [27] Li, X., Oh, J., Wang, Y., Zhu, H.: The method of transformed angular-basis function for solving the Laplace equation. *Eng. Anal. Bound. Elem.* **93**, 72–82 (2018)
- [28] Alves, C.J.S., Martins, N.F.M., Valtchev, S.S.: Trefftz methods with cracklets and their relation to BEM and MFS. *Eng. Anal. Bound. Elem.* **95**, 93–104 (2018)
- [29] Hong, H.-K., Chen, J.T.: Generality and Special Cases of Dual Integral Equations of Elasticity. *J. Chin. Soc. Mech. Eng.* **9**(1), 1–9 (1988)
- [30] Kuo, C.L., Yeih, W., Ku, C.Y., Fan, C.M.: The method of two-point angular-basis function for solving Laplace equation. *Eng. Anal. Bound. Elem.* **106**, 264–274 (2019)
- [31] Mura, T.: *Mathematical Theory of Dislocations*. American Society of Mechanical Engineers, New York (1969)
- [32] Lardner, R.W.: *Mathematical Theory of Dislocations and Fracture*. University of Toronto Press, Toronto (1974)
- [33] Leandro, P., Jr.: The tangential differential operator applied to a stress boundary integral equation for plate bending including the shear deformation effect. *Eng. Anal. Bound. Elem.* **36**(8), 1213–1225 (2012)
- [34] Liu, Y.J., Li, Y.X.: Revisit of the equivalence of the displacement discontinuity method and boundary element method for solving crack problems. *Eng. Anal. Bound. Elem.* **47**, 64–67 (2014)
- [35] Dundurs, J.: On the interaction of a screw dislocation with inhomogeneities. *Recent Adv. Eng. Sci.* **2**, 223–233 (1967)

J. T. Chen and S. K. Kao
Department of Harbor and River Engineering
National Taiwan Ocean University
Keelung
Taiwan

J. T. Chen
Department of Mechanical and Mechatronic Engineering
National Taiwan Ocean University
Keelung
Taiwan

J. T. Chen
Center of Excellence for Ocean Engineering
National Taiwan Ocean University
Keelung
Taiwan

J. T. Chen
Department of Civil Engineering
National Cheng Kung University
Tainan
Taiwan

J. T. Chen
Department of Civil Engineering
National Taiwan University
Taipei
Taiwan
e-mail: jtchen@mail.ntou.edu.tw

J. W. Lee
Department of Civil Engineering
Tamkang University
New Taipei City
Taiwan

(Received: June 11, 2022; revised: July 25, 2022; accepted: August 17, 2022)